Sigma Journal of Engineering and Natural Sciences
Web page info: https://sigma.yildiz.edu.tr
DOI: 10.14744/sigma.2024.00159

Research Article

# Effects of $SiO_2$ and $Al_2O_3$ nanoparticles on the properties of borogypsum containing mortar

**Meral YILDIRIM OZEN[1], Emek MOROYDOR DERUN[1,*]**

[1]*Department of Chemical Engineering, Yildiz Technical University, İstanbul, 34220, Türkiye*

## ARTICLE INFO

*Article history*
Received: 06 August 2023
Revised: 08 October 2023
Accepted: 28 October 2023

**Keywords:**
Borogypsum; Cement Mortar; Nanoparticle; Nano-$SiO_2$; Nano-$Al_2O_3$

## ABSTRACT

This study aimed to investigate the effects of nano-$SiO_2$ and nano-$Al_2O_3$ on the physicochemical and mechanical properties of mortars containing borogypsum. The mortars were modified by incorporating 0.2-1% nano-$SiO_2$ and 0.5-2.5% nano-$Al_2O_3$. Various analysis methods were applied to the nano-modified samples to observe changes in the fresh and hardened features of the mortars. The results showed that the nanoparticles used could not promote the setting of the mortars. The highest compressive strength of 67 MPa was achieved when 1% nano-$Al_2O_3$ was used. Adding 0.4% nano-$SiO_2$ resulted in the highest flexural strength of 9.13 MPa. Supporting the water absorption test, SEM and BET morphologic analyses showed that nano-$SiO_2$ was more effective in developing a denser microstructure than nano-$Al_2O_3$. The findings of the thermal analysis suggest that substituting nanoparticles in borogypsum-containing mortars could not decrease the unreacted CH ratio during the hydration under the studied conditions.

**Cite this article as:** Yıldırım Ozen M, Moroydor Derun E. Effects of $SiO_2$ and $Al_2O_3$ nanoparticles on the properties of borogypsum containing mortar. Sigma J Eng Nat Sci 2024;42(6):1923–1932.

## INTRODUCTION

In recent decades, the application of nanotechnology in construction materials to improve mechanical and chemical stability has gained importance. Generally, nanotechnological approaches aim to make superficial and intrinsic features more durable. The primary motivation for using nanoparticles in mortar blends is to use them as fillers for voids and as nuclei for hydration reactions to obtain superior properties [1-2]. Although there are some challenges in determining the appropriate amount and dispersion method, nanoparticles have significant potential for developing engineering properties of construction materials [1].

The feasibility of using several types of nanoparticles has been investigated in previous studies. The most commonly used nanoparticles are nano-$SiO_2$ [3-6], nano-$Al_2O_3$ [7-8], nano-$TiO_2$ [9-11], and nano-$Fe_2O_3$ [12].

Although the nanoparticles mentioned above are usually incorporated into mortar blends with industrial wastes of fly ash [3, 13-15] and blast furnace slag [16-17], there have been no studies on the coexistence of borogypsum with nano-$SiO_2$ and nano-$Al_2O_3$ in cement mortars. Borogypsum is industrial waste produced during boric acid production from colemanite and sulfuric acid reactions. Using borogypsum as a mineral admixture can help reduce

*Corresponding author.
*E-mail address: moroydor@yildiz.edu.tr

*This paper was recommended for publication in revised form by Editor-in-Chief Ahmet Selim Dalkilic*

the disposal of this industrial waste and turn it into an alternative supplementary cementitious material [18].

To the best of our knowledge, there is a lack of studies that have explored the characteristics of borogypsum mortars incorporating nano-$SiO_2$ and nano-$Al_2O_3$ despite the widespread investigation of borogypsum as industrial waste in civil engineering applications. The primary goal of this study was to assess the impact of borogypsum in mortar compositions when combined with nano-$SiO_2$ and nano-$Al_2O_3$ and to examine their interactions. Given that the presence of boron tends to extend the setting time, it is paramount to investigate how the utilization of nanoparticles influences various properties of the resulting mortars. To fulfill this objective, a series of mechanical tests and instrumental analyses were conducted on mortars cured for 3, 7, and 28 days. The microstructural assessment encompassed water absorption testing, scanning electron microscope (SEM) observation, and BET (Brunauer-Emmett-Teller) analysis.

## MATERIALS AND METHODS

### Materials

The industrial waste of borogypsum, supplied by Bandırma Boron Works (Eti Maden, Balıkesir, Turkey), was used instead of gypsum. XRD identified borogypsum (BJ), and according to the XRD results, borogypsum contained gypsum ($CaSO_4 \cdot 2H_2O$, powder diffraction file (PDF) no:00-006-0046) and calcium borate hydrate ($Ca_2B_{10}O_{17} \cdot 5H_2O$, pdf no:00-022-0146) [19]. Due to the chemical composition of borogypsum, clinker was used as the binder material and was provided by the Akcansa Cement Factory, Istanbul, Turkey. The fine aggregate of CEN standard sand conforming to EN 196-1 was [20] obtained from Limak Trakya Cement (Kırklareli, Turkey). Sigma Aldrich and Merck Chemicals supplied $SiO_2$ and $Al_2O_3$ nanoparticles, and their $S_{BET}$ were 175-225 $m^2/g$ and 120-190 $m^2/g$, respectively. The chemical compositions of the ingredients are listed in Table 1 [19]. A polycarboxylic ether-based superplasticizer admixture (SP) (MasterGlenium®51, BASF Turkey) inhibited nanoparticle agglomeration.

**Table 1.** The chemical compositions of the ingredient [19]

| Composition (%) | Clinker | Borogypsum |
|---|---|---|
| $SiO_2$ | 14.0 | 4.1 |
| $Al_2O_3$ | 3.0 | - |
| $Fe_2O_3$ | 4.7 | 1.0 |
| CaO | 76.5 | 45.1 |
| $SO_3$ | - | 48.7 |
| MgO | - | - |
| $B_2O_3$ | - | 1.1 |

### Preparation of Specimens

A total of 10 different cement mortars with different amounts of nano-$SiO_2$ and nano-$Al_2O_3$ were prepared (Table 2). In addition, the reference mixture was prepared without nanoparticles, whereas the clinker in the other mortars was partially replaced with nano-$SiO_2$ and nano-$Al_2O_3$. The quantities of nanoparticle substitutions were established at 0.2-1% for $SiO_2$, and 0.5-2.5% for $Al_2O_3$, derived from preliminary experiments wherein a range of nanoparticle quantities was examined, and the most favorable intervals were selected with respect to rheological and mechanical characteristics. All mortars with a water-to-cement ratio of 0.4 and a binder-to-sand ratio of 3.0 were prepared, and the SP ratio was kept constant at 0.50% of the binder. In preliminary studies, based on the literature [18, 21], several ratios of borogypsum replaced binder materials, and 3% was determined as the optimum ratio in terms of physical and mechanical features.

The reference mixture was prepared according to the EN 196-1 standard [20]. For the preparation of nanoparticle-containing mortars, a different pathway was followed: The mixing water, SP, and nanoparticle were mixed and stirred at 500 rpm for 5 minutes. This blend was combined with clinker, borogypsum, and sand. After stirring for 5 minutes at high speed, the mortars were molded in 40x40x160-mm three-cell prismatic molds. Also, some parts of the mortars were placed into 40x40x40-mm cubes for the water absorption test. Next, the molds were kept in a test cabinet (Nuve TK 120, Turkey) at 20±2 °C and 90% relative humidity. After 24 h, the mortars were removed from the molds and cured in tap water until testing.

### Test Procedure

Several tests were conducted on fresh and hardened nano-modified mortars to investigate their properties based on the nanoparticle type and ratio. TS EN 480-2 was followed to observe the change in the setting time. The initial and final setting times were determined by measuring the penetration

**Table 2.** Mixture proportions of cement mortars

| Mixture | Clinker (%) | BJ (%) | $SiO_2$ (%) | $Al_2O_3$ (%) |
|---|---|---|---|---|
| Control | 97.0 | 3 | - | - |
| BJ-S-1 | 96.5 | 3 | 0.2 | - |
| BJ-S-2 | 96.0 | 3 | 0.4 | - |
| BJ-S-3 | 95.5 | 3 | 0.6 | - |
| BJ-S-4 | 95.0 | 3 | 0.8 | - |
| BJ-S-5 | 94.5 | 3 | 1.0 | - |
| BJ-A-1 | 96.5 | 3 | - | 0.5 |
| BJ-A-2 | 96.0 | 3 | - | 1.0 |
| BJ-A-3 | 95.5 | 3 | - | 1.5 |
| BJ-A-4 | 95.0 | 3 | - | 2.0 |
| BJ-A-5 | 94.5 | 3 | - | 2.5 |

depth of the needle of the Vicat apparatus [21]. Compressive and flexural strength tests were performed according to the procedures described in the EN 196-1 standard [20] at 3, 7, and 28 days. The crystalline phases of 28 days cured cement mortars were identified using XRD (PANalytical B.V., Almelo, The Netherlands) in the pattern range of 5–90°. The samples were then finely ground to a final particle size of 90 μm. The samples were identified using inorganic crystal structure database (ICSD) patterns. Fourier transform infrared (FT-IR) spectroscopy (Perkin Elmer Spectrum One, MA, USA) was used to analyze the amorphous phases in the mortar matrix and the crystalline phases in the crystalline matrix. The vibrational properties of the hydration products in the optimum samples after 28 days of curing were observed in the 450–4000 $cm^{-1}$ range. The BET method and water absorption test were used to investigate the effects of nanoparticles on the mortars' pore structure. The samples' $S_{BET}$ and total pore volume were determined by nitrogen ($N_2$) adsorption on a Micromeritics ASAP 2020 instrument. Before analysis, the finely ground samples were degassed under a vacuum at 105 °C. The BET analysis relies on empirically establishing the connection between the pressure of $N_2$ in equilibrium with a mortar surface and the volume of gas adsorbed at that specific pressure on the surface [22]. Water absorption tests of the mortars were performed according to the BS 1881-122 standard [23]. The mortars were maintained in an incubator at 105 °C for 72 h. After removal from the incubator and cooling in a dry airtight vessel, the initial weights of the mortar samples were recorded. Following cumulative immersion periods of 10, 30, 60, and 120 min into tap water, the absorbed water percentage of the samples was calculated. Three samples were employed to assess each mortar's mechanical characteristics and water absorption capacity. The microstructure of the mortars cured for 28 days was observed using a scanning electron microscope (ZEISS EVO LS 10) after converting the samples into small fragments.

Thermal analyses of the mortars were performed using a PerkinElmer Diamond TG/DTA instrument. The samples were heated from 30 to 1000 °C at a 10 °C/min heating rate under a $N_2$ atmosphere. Thermogravimetric analysis ensures the determination of the quantity of CH, which indicates the hydration progress. The CH percentage was calculated from the start and end points of the CH decomposition (Equation 1).

$$CH(\%) = WL_{CH}(\%) \times \frac{MW_{CH}}{MW_H} \quad (1)$$

In Equation 1, $WL_{CH}$ is the weight loss because of the CH decomposition; $MW_{CH}$ and $MW_H$ are CH and water molecular weights, respectively [24-25].

## RESULTS AND DISCUSSION

### Setting Time of Mortars

The setting time results for the mortars are shown in Figure 1. Contrary to most of the studies in the literature, both nanoparticles increased the setting time of mortars for all addition ratios. Many studies have investigated the effects of borogypsum on the setting properties of cement mortars, and it has been proven that borogypsum shows set-retarding properties [26-27]. However, the nano-modification did not show development in the setting features of the mortars. As shown in Figure 1, when the initial setting time of the nanoparticle-containing mortars was similar, the nano-$Al_2O_3$ incorporation caused a remarkable difference in the final setting time. In the studies by Heikal et al., using $SiO_2$ and $Al_2O_3$ nanoparticles delayed the setting time when they were used with the superplasticizer. These

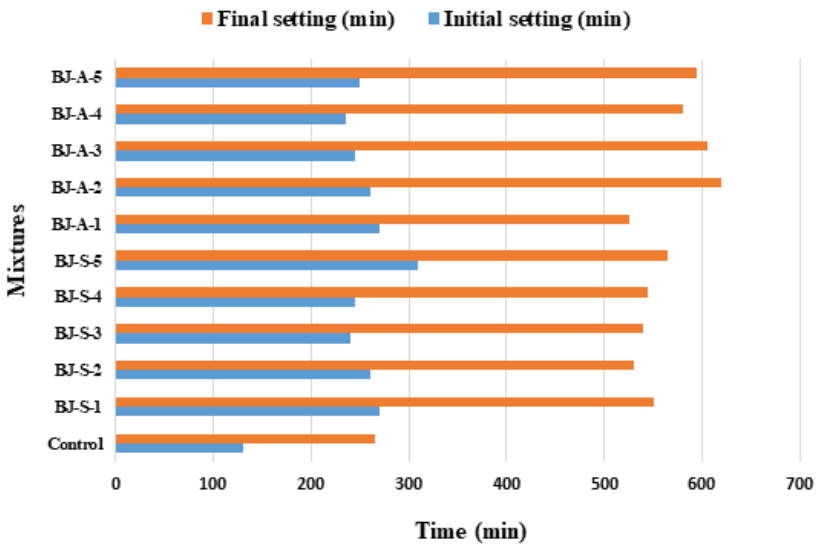


**Figure 1.** Setting time of mortars.

results were explained by the presence of a superplasticizer and the mixing procedure of nanoparticles and superplasticizers [28-29]. Similar to these studies, especially for the increased nanoparticle ratios, the presence of both the superplasticizer and borogypsum had a combined effect on set-retarding. They did not allow nanoparticles to show their pozzolanic activity effectively.

**The Compressive and Flexural Strength of Mortars**

The compressive strength development of the mortars with $SiO_2$ and $Al_2O_3$ nanoparticles is shown in Figure 2. The compressive strengths of 3-days cured mortars were compared, and it was observed that the compressive strength of the mortars decreased with increasing nanoparticle ratios.

As shown in Figure 2, 0.4% nano-$SiO_2$ usage improved the compressive strength of 28-days cured mortar as 1.94% of the reference value. However, increasing the nano-$SiO_2$ caused a remarkable decrease in compressive strength at all ages. The lack of uniform distribution of nano-$SiO_2$ can explain these results. When 1% nano-$Al_2O_3$ was incorporated into the mortars, the compressive strength of the 28-days cured mortar increased by 4.56%. Like the nano-$SiO_2$ replacement, nano-$Al_2O_3$ at higher ratios reduced the

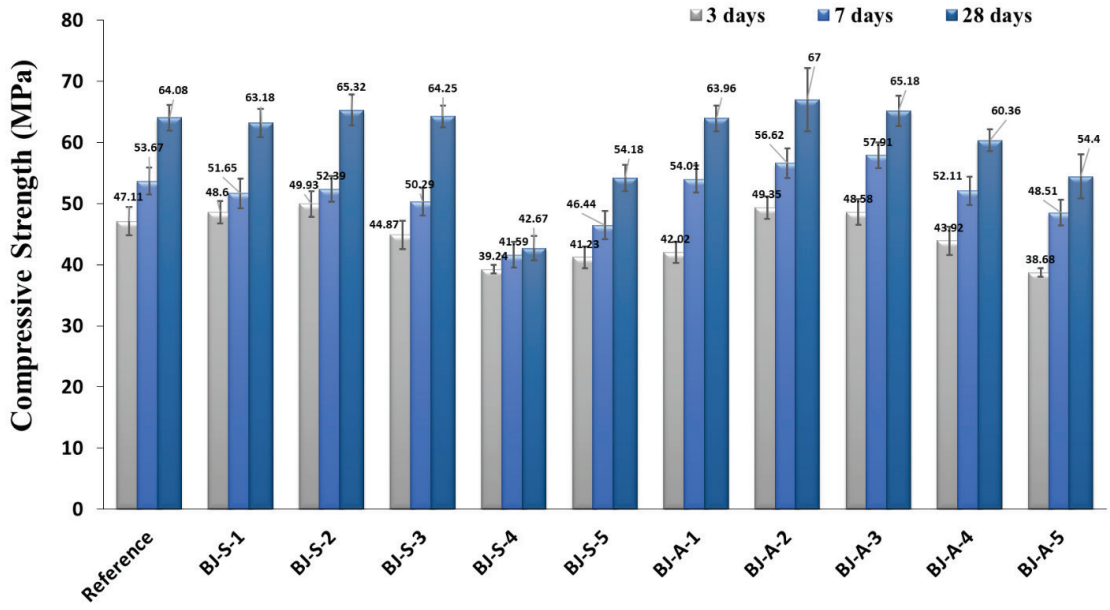


**Figure 2.** The compressive strength of mortars.

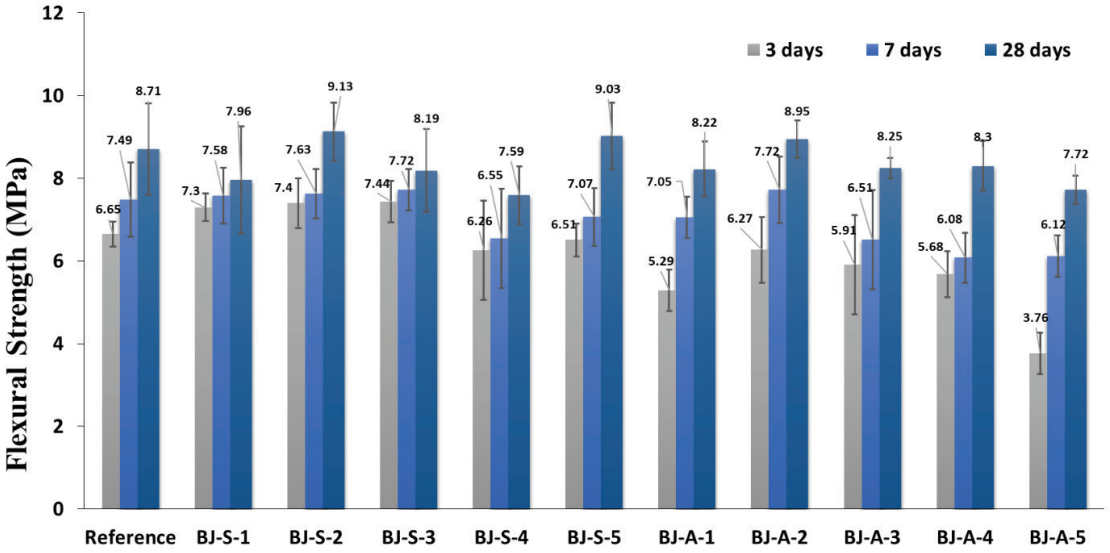


**Figure 3.** The flexural strength of mortars.

compressive strength. The compressive strength results showed that the agglomeration tendency of nano-$SiO_2$ and nano-$Al_2O_3$ caused a failure to obtain satisfactory results.

When the flexural strength of the mortars was investigated, it was observed that parallel to the compressive strength, the optimum nano-$SiO_2$, and nano-$Al_2O_3$ ratios were 0.4% and 1%, respectively (Figure 3). The flexural strength results of 3-days cured mortars showed that the usage of nano-$SiO_2$ up to 1.5% ensured higher development than the reference sample, which can be attributed to the nucleation effect of nano-$SiO_2$. On the other hand, the early-age strength of nano-$Al_2O_3$-containing mortars was lower than that of the reference. As a result of further curing, the 0.4% nano-$SiO_2$-containing mortar reached a flexural strength 4.82% higher than the reference sample. The flexural strength of 28-days cured nano-$Al_2O_3$-containing mortars showed that adding 1% nano-$Al_2O_3$ improved the flexural strength of mortars by 2.76% of the reference sample. The mechanical test results indicated that the combination of borogypsum and $Al_2O_3$ and $SiO_2$ nanoparticles could not improve the mechanical endurance of the mortars.

## XRD Results of Mortars

The crystalline phases in the mortar structure were determined using XRD analysis. The XRD patterns of the reference sample and selected mortars for each nanoparticle, which showed the highest mechanical strength, are presented in Figure 4.

According to the XRD analysis of the cement mortars, the main crystalline phase was quartz ($SiO_2$) with pdf number 00-046-1045, owing to the presence of sand. In addition to sand, portlandite ($Ca(OH)_2$) with pdf number 00-004-0733, calcium silicate hydrate ($Ca_{1.5}SiO_3{\cdot}xH_2O$) with pdf number 00-033-0306, and gismondine ($CaAl_2Si_2O_8{\cdot}4H_2O$) with pdf number 00-020-0452 were determined in the mortar composition.

For the BJ-A-2 sample, the peaks belonging to calcium alumina silicates (~68°) were higher than reference and nano-$SiO_2$-containing mortars. Also, different from the reference sample, the peak around 18° became sharper with the presence of nanoparticles.

## FT-IR Results of Mortars

The FT-IR spectra of the selected mortar samples are shown in Figure 5. The absorption band around 3640 $cm^{-1}$ is associated with O-H stretching vibrations of portlandite. The bands between 3440 $cm^{-1}$ - 2920 $cm^{-1}$ and around 1640 $cm^{-1}$ demonstrate O-H stretching and bending vibration of O-H due to the capillary water, respectively. The peaks detected at 2850 $cm^{-1}$, 1430 $cm^{-1}$, and 880 $cm^{-1}$ are attributed to the carbonation of $Ca(OH)_2$ with atmospheric $CO_2$ causes.

Calcium silicate hydrate (C-S-H) formation is characterized by intensified peaks at 1085 $cm^{-1}$ - 1030 $cm^{-1}$. In this region, peaks occurred due to the Si-O band's asymmetric stretching vibration. The peaks around 780 $cm^{-1}$ are related to the vibration of tetrahedral units of $AlO_4^{5-}$ which exist in the structure due to calcium alumina silicate (C-A-S) gel. The peaks observed at 696 $cm^{-1}$ indicate the symmetric bending of Si-O-Si. The out-of-plane Si-O bending causes bands around 520 $cm^{-1}$ when the peaks around 460 $cm^{-1}$ correspond to in-plane Si-O bending peaks. The obtained FT-IR spectra of the cement mortars align with the literature data [29-32].

## Scanning Electron Microscopy

SEM images of the reference sample and the optimum samples of BJ-S-2 and BJ-A-2 are shown in Figure 6. As shown in Figure 6, the addition of nanoparticles influenced the hydration of the mortars and initiated a change in the microstructure. The SEM images revealed that using nano-$SiO_2$ with borogypsum-containing mortar resulted in a denser and more compact microstructure than the reference and nano-$Al_2O_3$ blended mortar. The nano-$Al_2O_3$

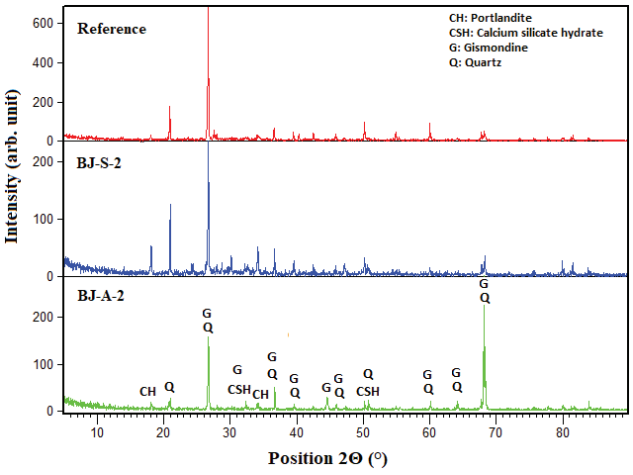


**Figure 4.** XRD patterns of selected samples.

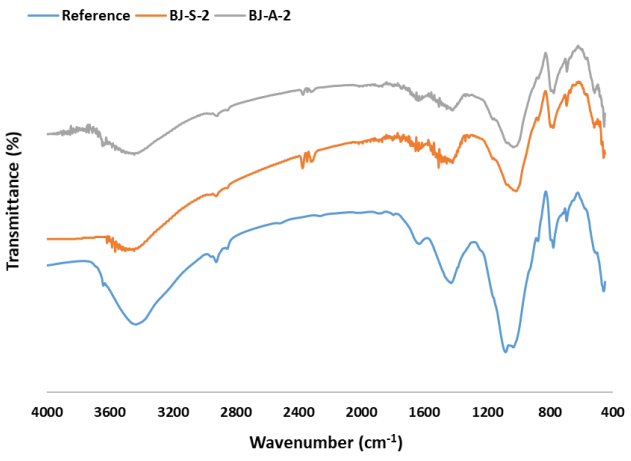


**Figure 5.** FT-IR spectra of selected samples.

containing mortar contains large amounts of ettringite needles. Furthermore, it had a more porous structure than the reference, which coincided with the water absorption values.

**BET Analysis Results of Mortars**

The BET-specific area and pore volume of the reference and nano-modified samples are listed in Table 3. When the $S_{BET}$ values of nano-$SiO_2$-containing mortars were investigated, it was clear that a significant improvement occurred in the specific surface of the mixtures when the nano-$SiO_2$ addition ratios were bigger than 0.2%, proving that there were smaller voids in the mortars. In addition, the specific pore volumes of the samples increased with increasing $S_{BET}$. These recent findings are consistent with those of Shih et al. [33]. According to BET analyses, the mortars' porosity did not significantly change when nano-$Al_2O_3$ was added to the mixtures. Furthermore, the denser microstructure in nano-$SiO_2$-containing mortars than those with nano-$Al_2O_3$ was demonstrated by measuring the higher mechanical resistance. The study by Seife et al. [34] yielded similar results, as it evaluated the effects of different activators on the mortar through BET tests and demonstrated a correlation between pore development and the material's mechanical strength.

**Water Absorption Results of Mortars**

The water absorption capacities of the nano-$SiO_2$ and nano-$Al_2O_3$-containing mortars are shown in Figures 7 and 8, respectively.

**Table 3.** BET-specific area and pore volume of samples

| Mix | SBET ($m^2/g$) | Pore volume ($cm^3/g$) |
|---|---|---|
| Reference | 1.1739 ± 0.0188 | 0.008533 |
| BJ-S-1 | 1.9089±0.0322 | 0.008568 |
| BJ-S-2 | 3.2464±0.0304 | 0.013539 |
| BJ-S-3 | 3.8543±0.0401 | 0.014667 |
| BJ-S-4 | 3.5187±0.0306 | 0.012835 |
| BJ-S-5 | 3.9842±0.0413 | 0.016548 |
| BJ-A-1 | 2.1251±0.0255 | 0.008948 |
| BJ-A-2 | 2.4169±0.0045 | 0.009775 |
| BJ-A-3 | 1.9678±0.0237 | 0.008557 |
| BJ-A-4 | 2.8730±0.0366 | 0.011116 |
| BJ-A-5 | 1.7259±0.0188 | 0.006371 |

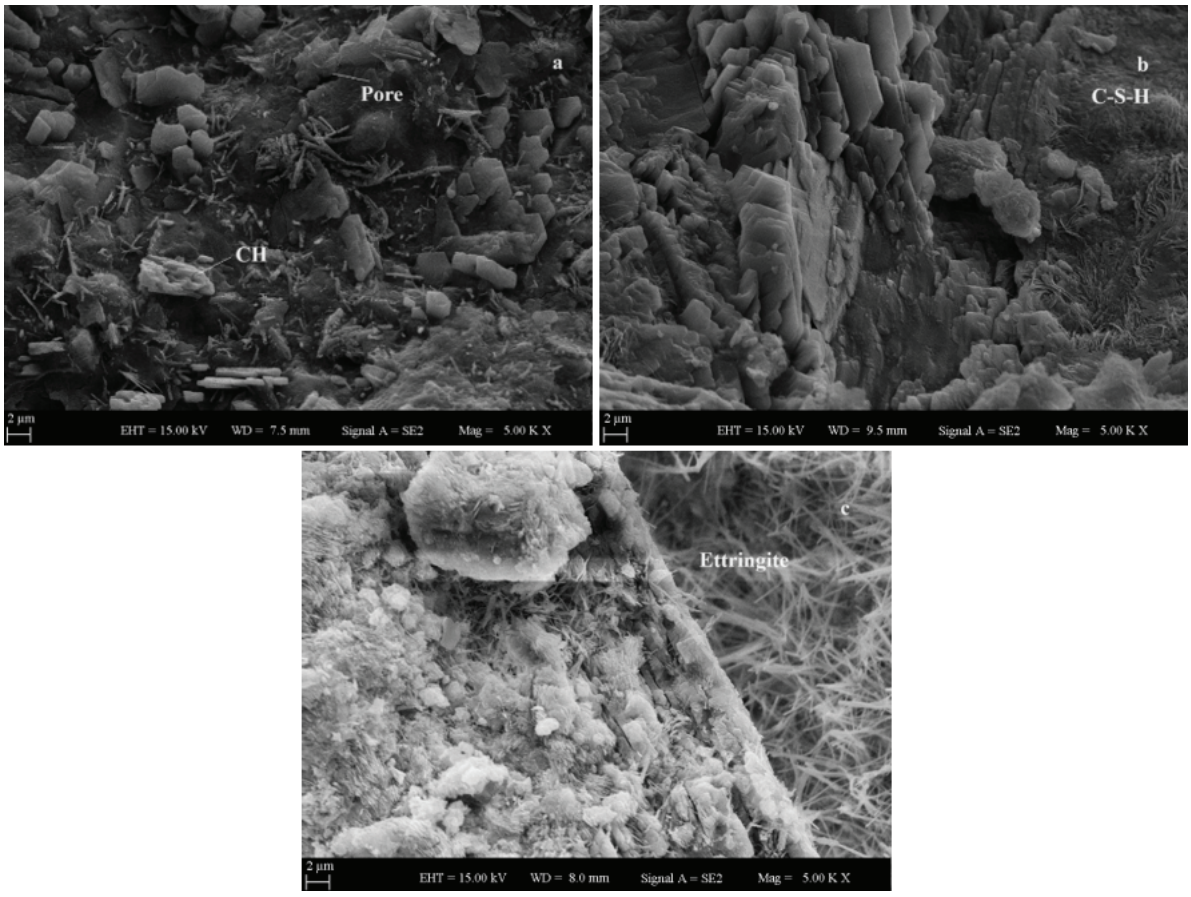


**Figure 6.** SEM images of selected samples (a. Reference, b. BJ-S-2, c. BJ-A-2).

As shown in Figure 7, using nano-$SiO_2$ in the mortar composition reduced water absorption. The compression between the mortars showed that the BJ-S-2 mortar absorbed 55% less water than the reference. The results demonstrate that adding nano-$SiO_2$ made the mortar matrix more compact and filled the pores, thus enhancing water absorption. On the contrary, the results showed that the percentage of water absorption was decreased by nano-$Al_2O_3$-containing mortars absorbing more water than the reference due to the increase in the porosity of the samples. The lack of water tightness of mortars incorporating nano-$Al_2O_3$ could be caused by the insufficient distribution of this nanoparticle, resulting in agglomeration and creating a more porous matrix [35].

As revealed by BET analysis results, the replacement of nano-$SiO_2$ supported the forming a denser structure and water tightness than nano-$Al_2O_3$. The observed decrease in water absorption by nano-$SiO_2$ corresponds to the results obtained in previous studies [36].

**Thermal Analysis Results of Mortars**

The DTA and DTG curves of selected mortars at 28 days of hydration are shown in Figure 9 and Figure 10, respectively. The thermal analysis curves, which are given for the temperature range of 200 °C and 800 °C, can be used for quantitative estimation of the CH content of the mortars. Considering the mass loss between 370°C and 500 °C, it is seen that the portlandite amount of the reference sample is lower than nanoparticle-incorporated samples besides the BJ-A-5 sample. The lack of primer hydration reactions possibly caused the lowest CH% of BJ-A-5. With the incorporation of nano-$SiO_2$, the decomposed CH amounts of the mortars changed between 6.55% and 8.81% when nano-$Al_2O_3$-containing mortars had a portlandite content of 4.08% - 8.03%. In addition, the thermal analysis curves

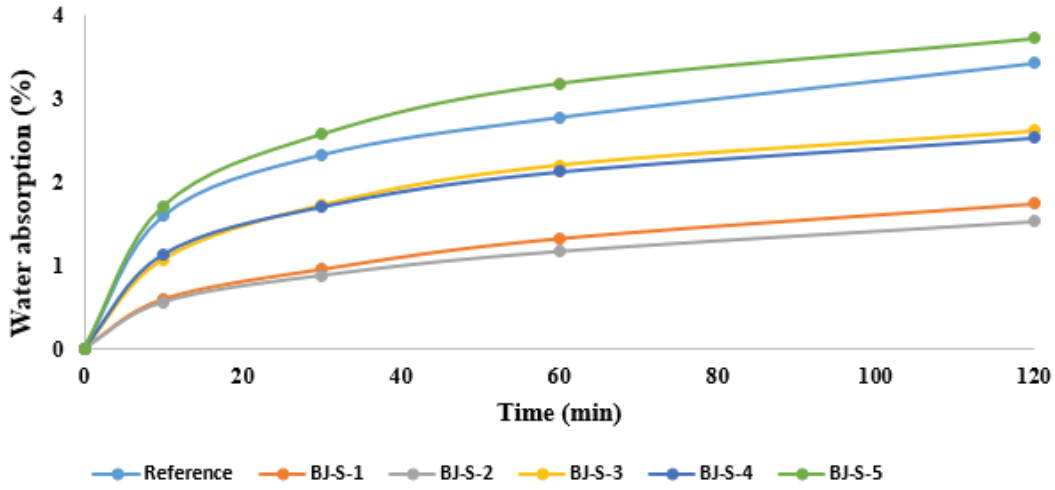


**Figure 7.** Water absorption percentage of nano-$SiO_2$-containing samples.

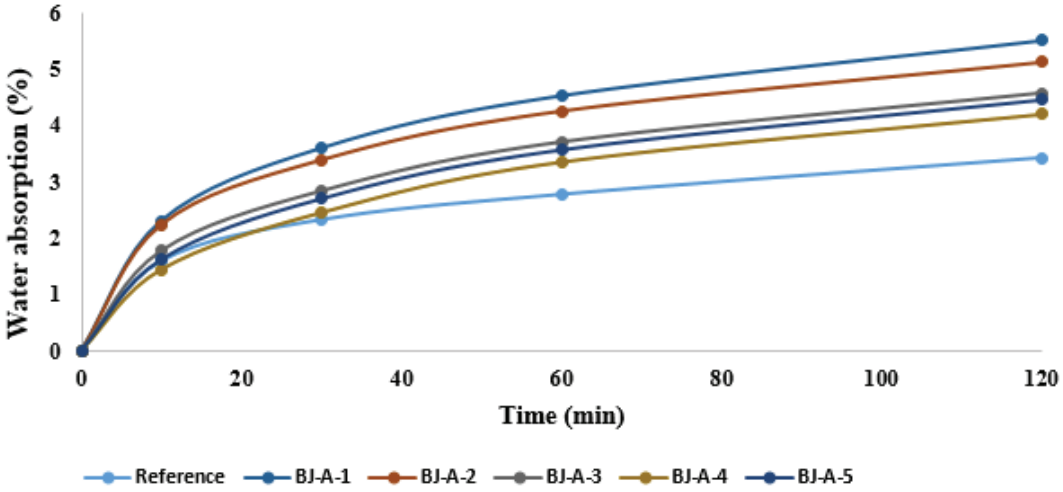


**Figure 8.** Water absorption percentage of nano-$Al_2O_3$-containing samples.

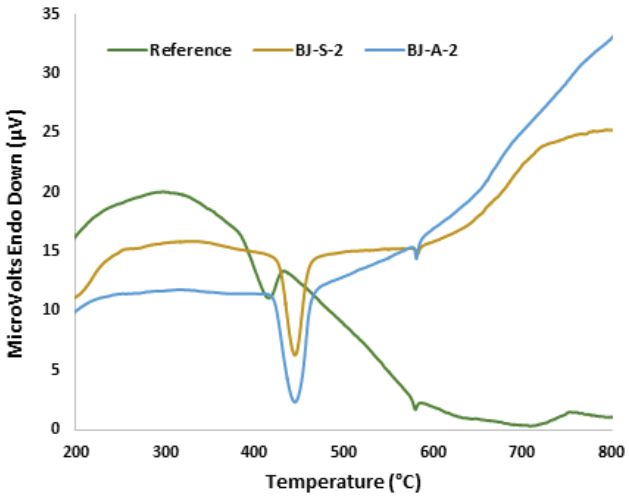


**Figure 9.** DTA curve of selected mortars.

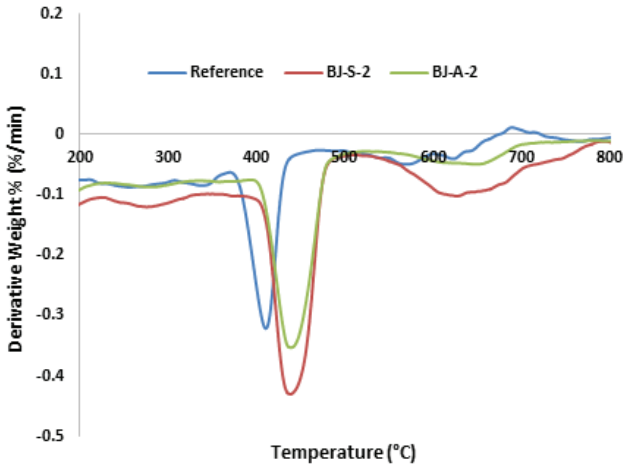


**Figure 10.** DTG curve of selected mortars.

**Table 4.** DTA/TG results of Ca $(OH)_2$ decomposition

| Mix | Initial Temperature (°C) | Final Temperature (°C) | CH content (%) |
|---|---|---|---|
| Reference | 370.78 | 436.79 | 4.49 |
| BJ-S-1 | 415.92 | 467.30 | 8.81 |
| BJ-S-2 | 421.46 | 464.50 | 8.65 |
| BJ-S-3 | 414.88 | 460.62 | 6.55 |
| BJ-S-4 | 415.14 | 462.18 | 6.59 |
| BJ-S-5 | 405.02 | 456.92 | 6.67 |
| BJ-A-1 | 403.74 | 479.16 | 6.63 |
| BJ-A-2 | 419.27 | 467.67 | 7.08 |
| BJ-A-3 | 407.22 | 456.49 | 6.26 |
| BJ-A-4 | 408.51 | 490.33 | 8.03 |
| BJ-A-5 | 403.28 | 464.47 | 4.08 |

demonstrate that adding nanoparticles shifts the initial decomposition temperature to higher values, which could be altered due to the reaction of the used nanoparticles with mortar and inhibiting portlandite from decomposition. When the mechanical and thermal analysis results are evaluated together, it is noticed that the nanoparticles used cannot ensure progress for secondary hydration reactions in which CH can be consumed.

## CONCLUSION

This study explores the effects of nano-$SiO_2$ and nano-$Al_2O_3$ on borogypsum-based mortars, addressing optimal concentrations, microstructural changes, and the impact on the hydration process, all representing valuable additions to the existing knowledge. From the obtained results, it can be stated that:

- Nanoparticles cannot enhance the acceleration of the setting of mortars. The combination of nanoparticles and borogypsum inhibited hydration.
- For all curing ages, increasing the dosages of nanoparticles caused a decrease in the compressive and flexural strengths. Nevertheless, compared with the reference sample, adding 0.4% nano-$SiO_2$ increased the compressive and flexural strengths by 1.94% and 4.82, respectively. Similarly, mortars containing 1% nano-$Al_2O_3$ had 4.56% and 2.76% higher compressive and flexural strengths, respectively.
- The SEM images, BET analysis, and water absorption results support the formation of a densified structure by nano-$SiO_2$ usage.
- According to the thermal analysis results, the nanoparticle-added samples include more portlandite than the reference sample, which can be attributed to the lack of secondary hydration reactions.

- Although using nanoparticles with supplementary cementitious materials could be practical and economical in many aspects, combining borogypsum with nano-$SiO_2$ and nano-$Al_2O_3$ could not achieve remarkable strength and durability.
- In further studies, changing the mixing method of nanoparticles can be investigated to obtain better results.

## ACKNOWLEDGMENTS

This research was supported by Yildiz Technical University Scientific Research Projects Coordination Department, with project number 2015-07-01-DOP04, and the authors wish to extend their sincere thanks to "The Scientific and Technological Research Council of Turkey (TÜBİTAK)" for its Ph.D. scholarship support.

## NOMENCLATURE

| | |
|---|---|
| *BJ* | Borogypsum |
| *CH* | $Ca(OH)_2$ |
| *DTA* | Differential Thermal Analysis |
| *DTG* | Derivative Thermogravimetric |
| *FT-IR* | Fourier transform infrared spectroscopy |
| *ICSD* | Inorganic crystal structure database |
| $MW_{CH}$ | Molecular weight of CH, g/cm$^3$ |
| $MW_H$ | Molecular weight of water, g/cm$^3$ |
| *pdf* | Powder diffraction file |
| $S_{BET}$ | BET surface area, m$^2$/g |
| *SP* | Superplasticizer admixture |
| TG | Thermogravimetric analysis |
| $WL_{CH}$ | Weight loss because of the CH decomposition, g |

## AUTHORSHIP CONTRIBUTIONS

Authors equally contributed to this work.

## DATA AVAILABILITY STATEMENT

The authors confirm that the data that supports the findings of this study are available within the article. raw data that support the finding of this study are available from the corresponding author, upon reasonable request.

## CONFLICT OF INTEREST

The author declared no potential conflicts of interest with respect to the research, authorship, and/or publication of this article.

## ETHICS

There are no ethical issues with the publication of this manuscript.

## REFERENCES

[1] Heikal M, Abdel-Gawwad HA, Ababneh FA. Positive impact performance of hybrid effect of nano-clay and silica nanoparticles on composite cements. Constr Build Mater 2018;190:508–516. [CrossRef]

[2] Zhan BJ, Xuan DX, Poon CS. The effect of nanoalumina on early hydration and mechanical properties of cement pastes. Constr Build Mater 2019; 202:169–176. [CrossRef]

[3] Wang J, Liu M, Wang Y, Zhou Z, Xu D, Du P, et al. Synergistic effects of nano-silica and fly ash on properties of cement-based composites. Constr Build Mater 2020;262:120737. [CrossRef]

[4] Mukharjee BB, Barai SV. Influence of nano-silica on the properties of recycled aggregate concrete. Constr Build Mater 2014;55:29–37. [CrossRef]

[5] Hani N, Nawawy O, Ragab KS, Kohail M. The effect of different water/binder ratio and nano-silica dosage on the fresh and hardened properties of self-compacting concrete. Constr Build Mater 2018;165:504–513. [CrossRef]

[6] Etli S. Evaluation of curing time for micro concrete mixes containing silica fume, nano-silica and fly ash. İstanbul Ticaret Üniv Fen Bilimleri Derg 2022;21:304–316. [CrossRef]

[7] Land G, Stephan D. Controlling cement hydration with nanoparticles. Cem Concr Comp 2015;57:64–67. [CrossRef]

[8] Farzadnia N, Ali AAA, Demirboga R. Characterization of high strength mortars with nano alumina at elevated temperatures. Cem Concr Res 2013;54:43–54. [CrossRef]

[9] Farzadnia N, Ali AAA, Demirboga R, Anwar MP. Characterization of high strength mortars with nano titania at elevated temperatures. Constr Build Mater 2013;43:469–479. [CrossRef]

[10] Dantas SRA, Serafini R, Cesar de Oliveira Romano R, Vittorino F, Loh K. Influence of the nano TiO2 dispersion procedure on fresh and hardened rendering mortar properties. Constr Build Mater 2019;215:544–556. [CrossRef]

[11] Ma B, Li H, Li X, Mei J, Lv Y. Influence of nano-TiO2 on physical and hydration characteristics of fly ash-cement systems. Constr Build Mater 2016;122:242–253. [CrossRef]

[12] Ahmed MA, Hassanean YA, Assaf KA, Shawkey MA. The effect of incorporation of ferrite nanoparticles on compressive strength and resistivity of self-compacting concrete. Open J Civ Eng 2015;5:131–138. [CrossRef]

[13] Oltulu M, Şahin R. Effect of nano-SiO2, nano-Al2O3 and nano-Fe2O3 powders on compressive strengths and capillary water absorption of cement mortar containing fly ash: A comparative study. Energy Build 2013;58:292–301. [CrossRef]

[14] Ibrahim RK, Hamid R, Taha MR, Fire resistance of high-volume fly ash mortars with nanosilica addition. Constr Build Mater 2012;36:779–786. [CrossRef]
[15] Servatmand A, Şimşek O. The determination of the optimum nano materials ratios in production of high performance mortar. J Polytechnic 2018;21:327–332.
[16] Heikal M, Al-Duaij OK, Ibrahim NS. Microstructure of composite cements containing blast-furnace slag and silica nanoparticles subjected to elevated thermally treatment temperature. Constr Build Mater 2015;93:1067–1077. [CrossRef]
[17] Liu M, Zhou Z, Zhang X, Yang X, Cheng X. The synergistic effect of nano-silica with blast furnace slag in cement based materials. Constr Build Mater 2016;126:624–631. [CrossRef]
[18] Sevim UK, Ozturk M, Onturk S, Bankir MB. Utilization of boron waste borogypsum in mortar. J Build Eng 2019;22:496–503. [CrossRef]
[19] Yildirim M, Derun EM. The influence of CuO nanoparticles and boron wastes on the properties of cement mortar. Mater Construc 2018;68:e161. [CrossRef]
[20] TS EN 196-1 Methods of testing cement - Part 1: Determination of strength, 2009.
[21] Kunt K, Dur F, Ertınmaz B, Yıldırım M, Moroydor Derun E, Pişkin S. Utilization of boron waste as an additive for cement production. CBÜ Fen Bil Derg 2015;11:383–389. [CrossRef]
[22] TS EN 480-2 Admixtures for concrete, mortar and grout - Test methods - Part 2: Determination of setting time 2008.
[23] Skalny J, Hearn N. Surface Area Measurements, in: V.S. Ramachandran, J.J. Beaudoin (Eds.), Handbook of Analytical Techniques in Concrete Science and Technology. New York, USA: Noyes Publications; 127–159, 2001. [CrossRef]
[24] BS 1881-122 Testing concrete: Method for determination of water absorption 2011.
[25] Vedalakshmi R, Sundara AR, Palaniswamy N. Identification of various chemical phenomena in concrete using thermal analysis. Indian J Chem Technol 2008;15:388–396.
[26] Ramachandran VS. Thermal Analysis, in: V.S. Ramachandran, J.J. Beaudoin (Eds.), Handbook of Analytical Techniques in Concrete Science and Technology. New York, USA: Noyes Publications; 127–159, 2001. [CrossRef]
[27] Boncukcuoğlu R, Yılmaz MT, Kocakerim MM, Tosunoğlu V. Utilization of borogypsum as set retarder in Portland cement production. Cem Conc Res 2002;32:471–475. [CrossRef]
[28] Kavas T, Olgun A, Erdogan Y. Setting and hardening of borogypsum-Portland cement clinker-fly ash blends. Studies on effects of molasses on properties of mortar containing borogypsum. Cem Conc Res 2004;35:711–718. [CrossRef]
[29] Heikal M, Abd El Aleem S, Morsi WM. Characteristics of blended cements containing nano-silica. HBRC J 2013;9:243-255. [CrossRef]
[30] Heikal M, Ismail MN, Ibrahim NS. Physico-mechanical, microstructure characteristics and fire resistance of cement pastes containing Al2O3 nanoparticles. Constr Build Mater 2015;91:232-242. [CrossRef]
[31] Barbhuiya S, Mukherjee S, Nikraz H. Effects of nano-Al2O3 on early-age microstructural properties of cement paste. Constr Build Mater 2014;52:189-193. [CrossRef]
[32] Li F, Liu J. An experimental investigation of hydration mechanism of cement with silicane. Constr Build Mater 2018;166:684-693. [CrossRef]
[33] Govindarajan D, Gopalakrishnan R. Spectroscopic studies on Indian Portland cement hydrated with distilled water and sea water. Front Sci 2012;1:21-27. [CrossRef]
[34] Horgnies M, Chen JJ, Bouillon C. Overview about the use of Fourier Transform Infrared spectroscopy to study cementitious materials. WIT Trans Eng Sci 2013;77:251-262. [CrossRef]
[35] Shih JY, Chang TP, Hsiao TC. Effect of nanosilica on characterization of Portland cement composite. Mat Sci Eng A 2006;424:266-274. [CrossRef]
[36] Seifi S, Levacher D, Razakamanantsoa A, Sebaibi N. Microstructure of dry mortars without cement: specific surface area, pore size and volume distribution analysis. Appl Sci 2023;13:5616. [CrossRef]
[37] Mohseni E, Mehdizadeh Miyandehi B, Yang J, Yazdi MA. Single and combined effects of nano-SiO2, nano-Al2O3 and nano-TiO2 on the mechanical, rheological and durability properties of self-compacting mortar containing fly ash. Constr Build Mater 2015;84:331-340. [CrossRef]
[38] Du H, Du S, Liu X. Durability performances of concrete with nano-silica. Constr Build Mater 2014;73:705-712. [CrossRef]